Prediction of Absorbed Dose to Normal Organs in Thyroid Cancer Patients Treated with ^{131}I by Use of ^{124}I PET and 3-Dimensional Internal Dosimetry Software

Katherine S. Kolbert[1], Keith S. Pentlow[1], Joel R. Pearson[1], Arif Sheikh[2], Ronald D. Finn[2], John L. Humm[1], and Steven M. Larson[2]

[1]*Department of Medical Physics, Memorial Sloan-Kettering Cancer Center, New York, New York; and* [2]*Department of Radiology, Memorial Sloan-Kettering Cancer Center, New York, New York*

The objective of this work was to determine normal organ ^{131}I dosimetry in patients undergoing radioiodide therapy for thyroid cancer by use of serial scanning with ^{124}I PET. **Methods:** A total of 26 patients who had papillary and follicular metastatic thyroid cancer and who were already enrolled in a Memorial Sloan-Kettering Cancer Center ^{131}I thyroid cancer protocol were selected for this study. Imaging before ^{131}I therapy consisted of multiple, whole-body ^{124}I PET studies over a period of 2–8 d, an ^{18}F-FDG PET scan and, for some, a diagnostic CT scan. With a set of in-house–developed software tools (3-dimensional internal dosimetry [3D-ID] and Multiple Image Analysis Utility [MIAU]), the following procedures were performed: all PET emission and transmission and CT image sets were aligned; half-life–corrected tomographic images of ^{131}I activity were integrated voxel by voxel to produce cumulated ^{131}I activity images; and the latter images were, in turn, convolved with a ^{131}I electron–photon point kernel to produce images of ^{131}I dose distribution. Cumulated activity values and calculated residence times obtained from our patient-specific dosimetry software (3D-ID) were used as inputs to OLINDA, and volume difference–adjusted comparisons were made between the mean dose estimates. **Results:** With 3D-ID, dose volume histograms and mean doses were calculated for 14 organs, and results were expressed in Gy/GBq. The highest mean dose, 0.26 Gy/GBq, was seen in the right submandibular gland, whereas the lowest mean dose, 0.029 Gy/GBq, was seen in the brain. **Conclusion:** This is the first comprehensive study of normal organ dosimetry in patients by use of a quantitative tomographic imaging modality.

Key Words: ^{131}I normal organ dose; thyroid cancer; ^{124}I PET; radioimmunotherapy

J Nucl Med 2007; 48:143–149

The intent of this study was to perform retrospective patient-specific, normal organ dosimetry for ^{131}I in patients with papillary and follicular metastatic thyroid cancer by use of multiple ^{124}I PET NaI scans to provide 3-dimensional kinetic voxel data. Dose calculation in the past most commonly relied on MIRD methods (*1*), which use standardized anatomic models to provide the basis for calculating doses. An in-house–developed software package, 3-dimensional internal dosimetry (3D-ID) (*2–5*), allows us to use patient-specific tomographic PET images of activity distribution for calculating doses. The 3D-ID software was used to generate the normal organ doses reported in this article but was not used to make decisions concerning therapeutic activities required for optimal therapy. The use of ^{124}I as a tracer for ^{131}I was previously demonstrated (*6,7*) and, in the present study, PET provided the quantitative basis (*8,9*) for dose calculation. The methodology used in the present study was previously described in some detail by Sgouros et al. (*4*), who used the combination of 3D-ID and ^{124}I PET to generate dose estimates for 56 lesions in a subset of 15 thyroid cancer patients from the same patient cohort as that used in the present study.

Current practice at our institution is to treat patients in a euthyroid state with recombinant human thyroid-stimulating hormone (rhTSH). It is known that the biokinetics in such patients are different from those in patients in the traditional hypothyroid treatment state; in particular, whole-body clearance and blood clearance are faster (*10,11*). Therefore, the data reported here may be different from the data acquired from patients in a hypothyroid state.

MATERIALS AND METHODS

Patient Population

The patient population for this retrospective study was selected from Memorial Sloan-Kettering Cancer Center (MSKCC) patients who were already undergoing treatment for thyroid cancer and

Received Mar. 1, 2006; revision accepted Sep. 18, 2006.
For correspondence or reprints contact: Katherine S. Kolbert, MS, Department of Medical Physics, Memorial Sloan-Kettering Cancer Center, 1275 York Ave., New York, NY 10021.
E-mail: katherinenyc@att.net

who, in addition, were enrolled in a study evaluating the use of ^{124}I PET (*4*). During the period from 1999 to 2001, patients with known or suspected disease outside the neck, preferably with stage M1 disease, were considered for inclusion. In total, a group of 26 patients qualified to participate in the present study. Appropriate institutional review board approval was granted. However, data collection and analysis took place before Health Insurance Portability and Accountability Act regulations went into effect; therefore, no additional consent forms were used.

All patients in the study group had undergone total thyroidectomy by surgery and thyroid remnant ablation with ^{131}I. Before imaging and therapy, all patients were prepared with rhTSH (Thyrogen; Genzyme). Patients ranged in age from 30 to 87 y; 10 were women and 16 were men. Histologic and TNM data for the 26 patients are shown in Table 1. For 25 of the 26 patients, the lesion load varied from 1.41 to 105.38 g. A single patient had a lesion load totaling 722.22 g, 7 times higher than the next highest lesion load.

Imaging

The thyroid imaging protocol practiced at MSKCC includes several different imaging modalities. Most patients undergo diagnostic CT in the region of suspected disease. For the purpose of the present study, these image sets were used when available to define the target organ for which the dose was calculated. In addition, for all patients, ^{18}F-FDG PET scans and 3–5 ^{124}I PET scans were obtained over several days before ^{131}I therapy. Imaging was done with an Advance PET scanner (GE Healthcare) in the 2-dimensional (septa-in) mode for ^{68}Ge transmission scans. The ^{18}F-FDG PET scans were usually acquired 1 or 2 d before the administration of ^{124}I. Imaging was performed in a fasting and resting state 45–60 min after the injection of 555 MBq (15 mCi) of ^{18}F-FDG. Emission imaging typically consisted of 5 or 6 bed positions of 4 or 5 min each, covering part of the body from the maxilla to the upper thigh. Standard ordered-subset expectation maximization clinical software with segmented attenuation correction was used for image reconstruction. On each of the 2 d before ^{124}I imaging, patients were given an intravenous injection of rhTSH. Oral administration of 74−158 MBq of ^{124}I was done on what was defined as day 0, and serial images of the patients were obtained as logistics permitted. Patients were again imaged with the Advance PET scanner in the 2-dimensional mode, with the system now set to ^{124}I to compensate for the reduced positron abundance and different half-life. No other corrections were necessary. The imaged region typically ranged from the top of the head to the middle thigh, requiring up to 7 bed positions. Generally, imaging was performed at approximately 4−6, 20, and 44 h after tracer administration; in some cases, additional images were obtained at later times. Typical imaging times were 6 min per field for emission scans and 3 min per field for transmission scans. Images were again reconstructed with standard clinical software (ordered-subset expectation maximization) and segmented attenuation correction. In addition, blood samples and whole-body counts were obtained as required by the standard MSKCC thyroid imaging protocol for blood dosimetric evaluation (*12*).

TABLE 1
Demographic and Disease Characteristics of Patients Who Met Criteria for Study Inclusion

Characteristic	Value
Age (y)	
Mean (SD)	61.7 (15.4)
Median (range)	64 (30−87)
Gender, no. (%)	
Women	10 (38)
Men	16 (62)
Weight (kg)	
Mean (SD)	77.5 (17.3)
Median (range)	78 (53−117)
Height (cm)	
Mean (SD)	170.8 (10.8)
Median (range)	171.5 (152.4−188.0)
Histology, no. (%)	
Papillary	18 (69.2)
Follicular	8 (30.8)
TNM stage, no. (%)	
T0	0
T1	1 (3.9)
T2	7 (26.9)
T3	2 (7.7)
T4	13 (50.0)
Tx	3 (11.5)
N0	1 (3.8)
N1	19 (73.1)
Nx	6 (23.1)
M0	5 (19.2)
Mx	0
M1	21 (80.8)
Lesion load* (g)	
Mean (SD)	40.9 (42)
Median (range)	26.1 (1.41−105.38)

*Lesion load data do not include 1 patient with very high lesion load (see text).

Image Registration

An in-house–developed software package, Multiple Image Analysis Utility [MIAU] (*13,14*), was used to coregister the serial ^{124}I PET scans. For each set of serial ^{124}I images, 1 was chosen as the reference dataset. All subsequent ^{124}I images were registered to

TABLE 2
^{131}I Average Mean Dose by Organ, as Determined with 3D-ID and Serial ^{124}I PET Images

Organ	No. of patients in which organ could be identified	Dose (Gy/GBq), average mean ± SD
Brain	5	0.029 ± 0.01
Left parotid gland	23	0.19 ± 0.2
Right parotid gland	23	0.22 ± 0.2
Left submandibular gland	22	0.20 ± 0.2
Right submandibular gland	20	0.26 ± 0.2
Left lung	7	0.078 ± 0.03
Right lung	7	0.082 ± 0.03
Heart wall	11	0.079 ± 0.03
Heart chamber	11	0.11 ± 0.04
Liver	19	0.094 ± 0.06
Left kidney	21	0.10 ± 0.06
Right kidney	22	0.095 ± 0.04
Spleen	18	0.087 ± 0.04
Pancreas	5	0.12 ± 0.07

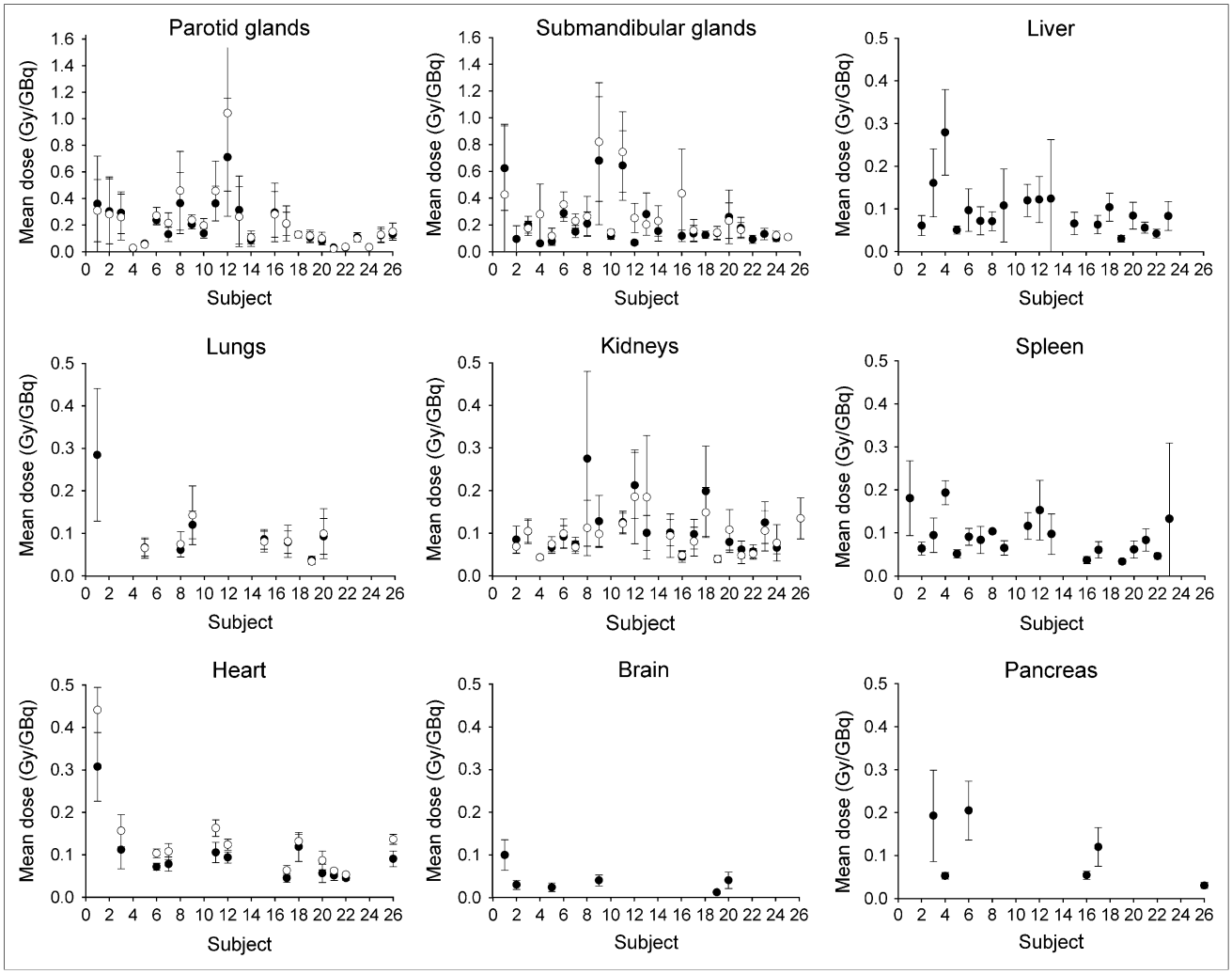

FIGURE 1. Mean ± SD dose for each organ and for each subject. Right and left organ pairs and heart chamber and wall are graphed together. Maximum value on *y*-axis for salivary glands is 1.6 Gy/GBq; maximum value on *y*-axis for all other organs is 0.5 Gy/GBq.

the reference image by use of a previously described semiautomatic landmark registration method (*14*) and, if necessary, a set of manual translations and rotations. No interpolation of activity values was performed to ensure that no voxel values were altered during the registration process. Because of the limitations imposed by allowing only rigid transformations, it was necessary to do multiple registrations for the same serial dataset with different reference body segments (e.g., thorax and pelvis) to ensure the alignment of those regions.

Available ^{18}F-FDG and CT image sets were registered to the ^{124}I PET reference image with the same registration techniques.

Generation of Cumulated ^{131}I Activity Images

To account for the half-life differences between ^{124}I, the imaging isotope, and ^{131}I, the dosimetry isotope, each voxel value was decay corrected to the time of the oral administration of ^{124}I and then decayed for ^{131}I to the appropriate time point. The resulting registered images of ^{131}I activity were then integrated on a voxel-by-voxel basis to generate single 3-dimensional images of cumulated activity (*14*).

Generation of Dose Images

With the 3D-ID software, the dose absorbed by each image voxel was calculated with a ^{131}I point kernel (*15*) generated by Monte Carlo simulation of photon spectrum transport through water and modified to account for the local deposition of electron energy (*2*). Because the density of soft tissue is generally considered to be approximately 1.0 g/cm^3, mass and volume are considered to be equivalent values when the point kernel is used for dosimetry in all organs except for the lungs (*2–5*). With a value of 0.3 g/cm^3 for the density of the lungs, the difference in tissue density can be compensated for by increasing the β-component of the self-dose 3-fold. With this method, there is a slight underestimation of the photon dose. An additional limitation of the point kernel method, as implemented in 3D-ID, is that no consideration is given to the attenuating effects of bone, leading to further small dose errors within and adjacent to bone tissue.

Organ Regions of Interest (ROIs)

Target organs were defined by drawing ROIs on the coregistered images from the image modality with which the organ of

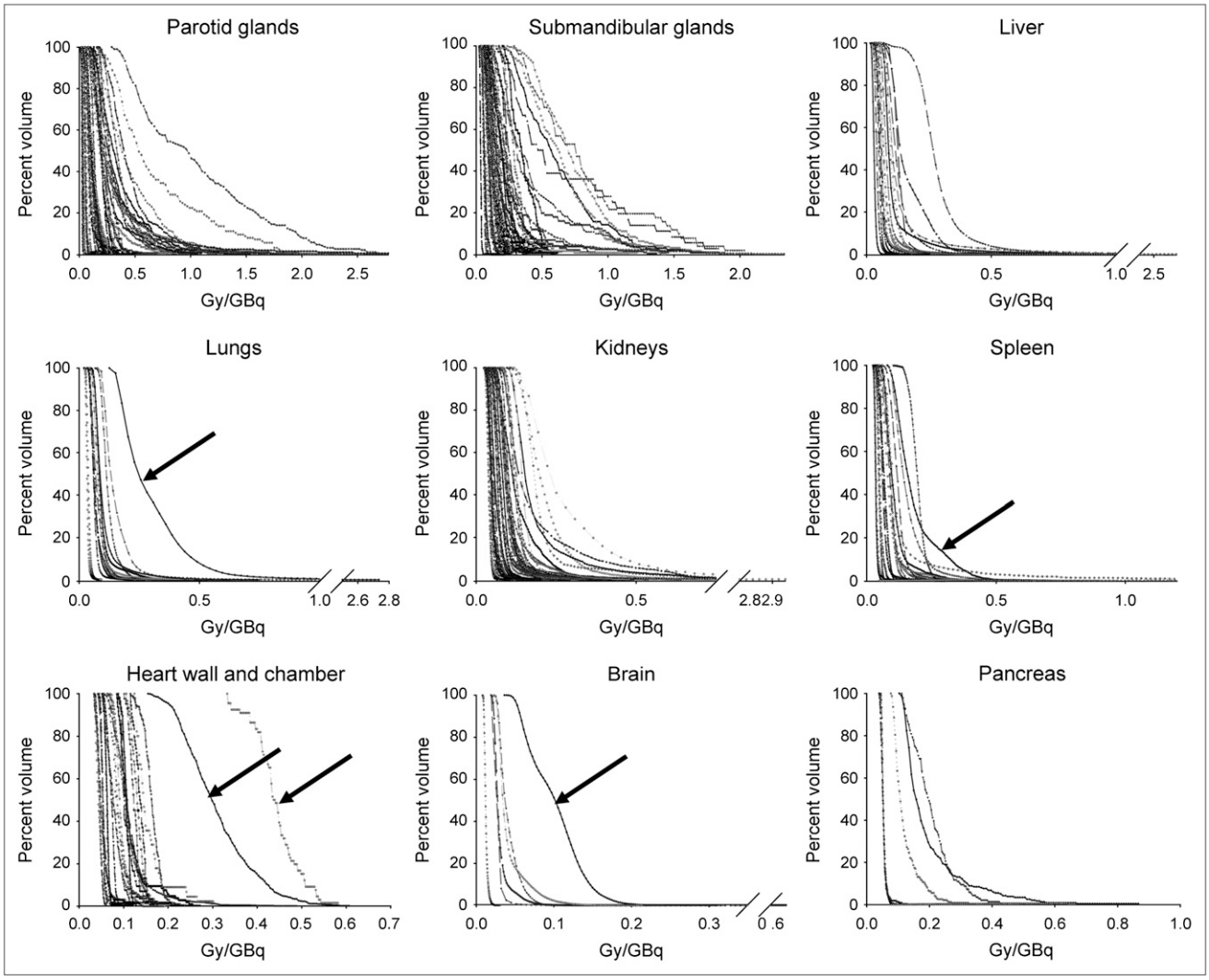

FIGURE 2. Integral DVHs by organ for each subject. *y*-Axis shows volume of organ (%) receiving at least the dose in Gy/GBq on *x*-axis. To show full range of doses and to demonstrate heterogeneity of distribution, range on *x*-axis varied from one organ group to the next. Arrows indicate DVHs for subject with high lesion load.

interest is best visualized. Although the intention was to use CT images for as much of the organ definition as possible, the CT images were acquired for clinical diagnostic purposes and therefore did not generally cover the whole body. Therefore, transmission images were used for the lungs; ^{18}F-FDG scans were used for the brain, salivary glands, heart, liver, kidneys, and spleen; and ^{124}I scans were used for the brain (seen as no uptake) and the salivary glands (if not seen on the ^{18}F-FDG scans). The CT images, when available, were used to define the region of the pancreas and to verify the locations of the liver, spleen, and kidneys. Any organ in which disease was present, as indicated by radiology reports, was rejected for this analysis, whose focus was to determine the radioiodine dose absorbed by normal organs.

Organ contours were manually drawn on each sequential axial slice with 3D-ID (*2,3*). With the 3D-ID software, coregistered images are displayed side by side so that voxel intensity information from both imaging modalities can be used while one is drawing contours. The drawing cursor appears in both images to assist in the identification of corresponding points. Contours are drawn on either image, and it is possible to switch back and forth between images during drawing. Region boundaries were drawn carefully to avoid including extraneous high-activity sources or areas subject to motion artifacts. Potential high-activity sources include the intestines, stomach, heart, and kidneys. Areas subject to motion artifacts are primarily near the heart or the lung–diaphragm–liver boundary.

The resultant target organ ROIs were transferred to the 3-dimensional dose distribution image sets for the calculation of mean organ doses and dose volume histograms (DVHs).

Other Methods for Dose Calculation

OLINDA (*16*), the recently published replacement code for MIRDOSE3 (*17*), was used to provide an independent and alternative method for calculating mean doses for comparison with 3D-ID–generated mean doses. The inputs to OLINDA consisted of residence times for each organ as defined by the sum of the values in 3D-ID–defined organ regions divided by the administered activity. The organ sizes of the phantom models used

by OLINDA were modified to reflect the actual size of the organ region as defined by 3D-ID, causing the β-components of the self-dose to be scaled linearly with respect to the ratio of the phantom to 3D-ID–defined organ masses and the photon components of the self-dose to be scaled with the two-thirds power of the ratio of the organ masses (*16*).

RESULTS

With the 3D-ID software, the radiation-absorbed dose was calculated for each organ for each patient in the study. Because of the ability of 3D-ID to generate a dose for each voxel, DVHs as well as mean doses were calculated and expressed in Gy/GBq of ^{131}I administered. In addition, the mean doses for each organ were averaged across patients to generate a single value, the average mean dose, for each organ.

A single subject (subject 1) in the study group of 26 subjects was found to have a dose to the brain (0.10 ± 0.04 [mean ± SD] Gy/GBq) more than 3 times that in any of the other subjects. As previously noted, this particular subject also had a 7-fold-higher lesion load (722 g) than the subject with the next highest lesion load (105 g). Given that iodine stays in metastatic thyroid cancer lesions longer than in normal tissue, it is reasonable to expect that the dose in non-organifying tissue will be higher in patients with large amounts of diseased tissue. For this reason, we removed data for subject 1 from the average mean dose calculation, so that the values shown in Table 2 do not include data for this subject. However, when mean doses for individual subjects are reported (Figs. 1 and 2), the mean doses for subject 1 are included.

In Table 2, the average mean dose is tabulated for each body organ. The number of patients in which the organ could be identified is also shown. This number is different from the total number of patients in the study because not all images covered the full extent required (head to middle thigh). If the organ was not visualized or was not identifiable in any of the images available for a particular study, no ROI was drawn for that organ. In addition, if an organ was identified as having disease, that organ was excluded from the mean dose calculation. Organ average mean doses ranged from a low of 0.029 ± 0.01 Gy/GBq in the brain to a high of 0.26 ± 0.2 Gy/GBq in the right submandibular gland.

In Figure 1, individual patient mean doses are grouped by organ for comparison of intraorgan variability. In Figure 2, DVHs that were generated from the voxel dose data are also grouped by organ. For the liver, lungs, heart, spleen, and brain, the shapes of the DVHs for most subjects indicate a homogeneous distribution. The kidneys, as might be expected, show greater heterogeneity. The apparent heterogeneity seen in the salivary glands is in part artifactual, attributable to their small size being comparable to the spatial resolution of the scanner. The subject with the high lesion load (subject 1) clearly received higher and more heterogeneous doses in the lungs, spleen, heart, and brain. (The liver dose was not calculated for this subject.) Of particular interest for radiation toxicity are the salivary glands, for which a small subset of the patients had doses extending up to values in excess of 1.5 Gy/GBq.

The average mean doses calculated for analogous organs with 3D-ID and OLINDA are shown in Table 3. These results demonstrate relatively close agreement between the patient-specific dosimetry performed here and the mean doses predicted for an organ size–adjusted, standard man by the U.S. Food and Drug Administration–approved OLINDA dosimetry package.

Blood doses derived from blood samples and whole-body counts obtained as part of the standard MSKCC thyroid imaging protocol (*12*) are tabulated in Table 4 and ranged from 0.05 to 0.18 Gy/GBq (median: 0.1 Gy/GBq), with a mean ± SD of 0.11 ± 0.03 Gy/GBq. Although agreement between these data and image-derived dose data for the heart is not always exact, the mean dose in both cases is 0.11 Gy/GBq, with only a very small variance in the SD.

DISCUSSION

The standard protocol at MSKCC for the treatment of patients with thyroid carcinoma involves surgical removal

TABLE 3
Comparison of Mean Doses Calculated with 3D-ID, OLINDA, and ICRP Model

Organ	No. of patients in which organ could be identified	Dose (Gy/GBq), average mean ± SD		
		3D-ID	OLINDA	ICRP
Brain	5	0.029 ± 0.01	0.031 ± 0.05	
Left lung	7	0.078 ± 0.03		
Right lung	7	0.082 ± 0.03		
Average lungs			0.091 ± 0.03	0.051
Liver	19	0.094 ± 0.06	0.084 ± 0.04	
Left kidney	21	0.10 ± 0.06		
Right kidney	22	0.095 ± 0.04		
Average kidneys			0.088 ± 0.03	0.1
Spleen	18	0.087 ± 0.04	0.075 ± 0.05	0.058
Pancreas	5	0.12 ± 0.07	0.14 ± 0.06	0.061

TABLE 4
Blood Dose Data*

Patient	Dose (Gy/GBq)	
	Measured in blood	Calculated by 3D-ID for heart chamber
1	0.27	0.44
2	0.093	
3	0.13	0.16
4	0.088	
5	0.13	
6	0.12	0.10
7	0.13	0.11
8	0.094	
9	0.10	
10	0.14	
11	0.17	0.16
12	0.15	0.12
13	0.12	
14	0.071	
15	0.10	
16	0.10	
17	0.095	0.063
18	0.18	0.13
19	0.052	
20	0.11	0.087
21	0.093	0.062
22	0.066	0.053
23	0.17	
24	0.079	
25	0.077	
26	0.13	0.14

*When patient with high lesion load was included in analysis, doses measured in blood and calculated by 3D-ID for heart chamber were as follows: mean (SD), 0.12 (0.05) and 0.14 (0.10) Gy/GBq, respectively; median (range), 0.11 (0.052−0.27) and 0.12 (0.053−0.44) Gy/GBq, respectively. When patient with high lesion load was not included in analysis, doses measured in blood and calculated by 3D-ID for heart chamber were as follows: mean (SD), 0.11 (0.03) and 0.11 (0.04) Gy/GBq, respectively; median (range), 0.10 (0.052−0.18) and 0.11 (0.053−0.16) Gy/GBq, respectively.

of the thyroid and then, typically, a therapy dose of ^{131}I to ablate any thyroid remnant and possible local–regional nodes (*18*). If there are distant metastases requiring further ^{131}I therapy, subsequent therapy doses are preceded by a dosimetry procedure to determine the maximum safe activity that can be administered (*12,19,20*). This procedure usually involves the administration of a test dose of 185 MBq of ^{131}I and then 4 d of blood and whole-body measurements, with a whole-body scan at 48–72 h. Previous attempts at predictive lesion dosimetry with planar imaging and SPECT have encountered several limitations; with planar imaging, there is uncertainty regarding active lesion dimensions, and with SPECT, the counting rate at diagnostic activity levels is inadequate for accurate quantification of the lesion uptake of ^{131}I. The advent of quantitative clinical PET and the availability of ^{124}I led to an investigative study of ^{131}I lesion dosimetry in which ^{124}I was substituted for ^{131}I in the dosimetry procedure and serial PET scans from the head to the pelvis were obtained at various times after administration (*4*). That dosimetry study yielded radioiodine uptake and clearance kinetics not only at the sites of thyroid disease but also for many of the normal organs for which radioiodine dosimetry with the accuracy of PET previously had not been performed.

Whereas the dosimetry data reported in the present study are primarily useful for patients undergoing therapy for thyroid disease, there is disagreement as to whether these data are applicable in another context, namely, providing approximate estimates of the dose from free iodide resulting from dehalogenation in patients undergoing ^{131}I-labeled antibody studies. The patients in the 2 groups differ in that patients in 1 group have normal thyroids whose function has been temporarily blocked, whereas patients in the other group have had their thyroids surgically removed, have received replacement thyroid hormone, and have additionally received 2 doses of rhTSH. Patients in both groups, however, are nominally euthyroid, with little or no active functional thyroid tissue. We are not aware of any experimental studies supporting the comparability of biokinetics under the 2 conditions, and such studies would, in practice, be very difficult to perform rigorously.

Iodide dosimetry data have been obtained with MIRD (*21*) and reported by the International Commission on Radiological Protection (ICRP) (*22*). The MIRD data were based on human tissue distribution data that were obtained from various sources and that were used as inputs to a model previously described by Berman et al. (*23*). The ICRP simplified the MIRD model with additional inputs from other sources. Data obtained with 3D-ID and the ICRP model for comparable organs are tabulated in Table 3. Johansson et al. (*24*) subsequently refined the ICRP model further. Edmonds and Smith also reported organ dose estimates obtained with MIRD and their previously described model (*25,26*). The ICRP and Edmonds and Smith allowed for 0% thyroid uptake; MIRD allowed a minimum of 5%. The absorbed doses quoted by Johansson et al. were for a thyroid uptake of 35%, although their model could be adjusted. The overall lists of organs considered in the various publications differ from each other and from the list used in the present study. However, when the same organs are considered and thyroid uptake values are similar, there is reasonable, although not exact, agreement between the present study (based on direct in vivo measurements of activity concentrations over time) and previous publications (based on models with tissue data and rate information from various sources). Specifically, the doses for the salivary glands, grouped together by Edmonds and Smith (0% thyroid uptake) and by Johansson et al. (30% thyroid uptake), were approximately 2-fold higher. The doses for the liver and lungs, as obtained with MIRD (5% thyroid uptake) and as reported by the ICRP (0% thyroid uptake), were more than 3-fold lower. Interestingly and in contrast, the comparison between 3D-ID and

OLINDA (Table 3) shows close agreement for average mean doses. This finding is to be expected, because the inputs to both OLINDA and 3D-ID were the same; organ masses in OLINDA were scaled to agree with patient organ masses in 3D-ID, and the same kinetic data were used.

The above-mentioned publications generally used a single mean value for each input parameter in their models. When the current data are examined in more detail, it is clear that there is considerable patient-to-patient variability in the mean doses for each organ, as exemplified in Figure 1. Because 3D-ID considers the activity in the entire body, from all organs and tissues, as a source for a particular target region and is based on patient-specific geometry, as opposed to model-based approaches, this variability more closely represents the actual dose distribution.

CONCLUSION

Using a set of in-house–developed dosimetry software tools, 3D-ID and MIAU, we calculated mean absorbed doses and DVHs for 26 patients and for 14 organ systems. These data should prove useful in estimating normal organ doses for patients who are undergoing ^{131}I therapy for thyroid cancer.

ACKNOWLEDGMENTS

This work was supported in part by U.S. Department of Energy grants DE-FG02-86ER60407 and DE-4D0205ER64001, National Institutes of Health grant P50 CA 086438, the Laurent and Alberta Gerschel Foundation, and the Ludwig Trust.

REFERENCES

1. Loevinger R, Budinger TF, Watson EE. *MIRD Primer for Absorbed Dose Calculations.* New York, NY: Society of Nuclear Medicine; 1991:1–17.
2. Kolbert KS, Sgouros G, Scott AM, et al. Implementation and evaluation of patient-specific three-dimensional internal dosimetry. *J Nucl Med.* 1997;38:301–308.
3. Sgouros G, Kolbert KS. The three-dimensional internal dosimetry software package 3D-ID. In: Zaidi H, Sgouros G, eds. *Therapeutic Applications of Monte Carlo Calculations in Nuclear Medicine.* Philadelphia, PA: Institute of Physics; 2002:249–258.
4. Sgouros G, Kolbert KS, Sheikh A, et al. Patient-specific dosimetry for ^{131}I thyroid cancer therapy using ^{124}I PET and 3-dimensional-internal dosimetry (3D-ID) software. *J Nucl Med.* 2004;45:1366–1372.
5. Sgouros G, Squeri S, Ballangrud AM, et al. Patient-specific, 3-dimensional dosimetry in non-Hodgkin's lymphoma patients treated with ^{131}I-anti-B1 antibody: assessment of tumor dose-response. *J Nucl Med.* 2003;44:260–268.
6. Flower MA, Schlesinger T, Hinton PJ, et al. Radiation dose assessment in radioiodine therapy, 2: practical implementation using quantitative scanning and PET, with initial results on thyroid carcinoma. *Radiother Oncol.* 1989;15:345–357.
7. Erdi YE, Macapinlac H, Larson SM, et al. Radiation dose assessment for I-131 therapy of thyroid cancer using I-124 PET imaging. *Clin Positron Imaging.* 1999;2:41–46.
8. Pentlow KS, Graham MC, Lambrecht RM, et al. Quantitative imaging of I-124 using positron emission tomography with applications to radioimmunodiagnosis and radioimmunotherapy. *Med Phys.* 1991;18:357–366.
9. Pentlow KS, Graham MC, Lambrecht RM, et al. Quantitative imaging of iodine-124 with PET. *J Nucl Med.* 1996;37:1557–1562.
10. Park S, Reynolds J, Brucker-Davis F. Diagnostic use of recombinant human TSH (rhTSH) vs. hypothyroidism [abstract]. *J Nucl Med.* 1996;37(suppl):15P.
11. Luster M, Sherman SI, Skarulis MC, et al. Comparison of radioiodine biokinetics following the administration of recombinant human thyroid stimulating hormone and after thyroid hormone withdrawal in thyroid carcinoma. *Eur J Nucl Med Mol Imaging.* 2003;30:1371–1377.
12. Furhang EE, Larson SM, Buranapong P, Humm JL. Thyroid cancer dosimetry using clearance fitting. *J Nucl Med.* 1999;40:131–136.
13. Kolbert KS, Sgouros G. Display and manipulation of SPECT and CT studies for radiolabeled antibody therapy [abstract]. *Cancer Biother Radiopharm.* 1998;13:302.
14. Kolbert KS, Hamacher KA, Jurcic JG, et al. Parametric images of antibody pharmacokinetics in Bi213-HuM195 therapy of leukemia. *J Nucl Med.* 2001;42:27–32.
15. Furhang EE, Sgouros G, Chui CS. Radionuclide photon dose kernels for internal emitter dosimetry. *Med Phys.* 1996;23:759–764.
16. Stabin MG, Sparks RB, Crowe E. OLINDA/EXM: the second-generation personal computer software for internal dose assessment in nuclear medicine. *J Nucl Med.* 2005;46:1023–1027.
17. Stabin MG. MIRDOSE: personal computer software for internal dose assessment in nuclear medicine. *J Nucl Med.* 1996;37:538–546.
18. Robbins RJ, Larson SM, Sinha N, et al. A retrospective review of the effectiveness of recombinant human TSH as a preparation for radioiodine thyroid remnant ablation. *J Nucl Med.* 2002;43:1482–1488.
19. Benua RS, Leeper RD. A method and rationale for treating thyroid carcinoma with the largest safe dose of I-131. In: Meideros-Neto GA, Gaitan E, eds. *Frontiers of Thyroidology.* Vol. II. New York, NY: Plenum; 1986:1317–1321.
20. Benua RS, Cicale NR, Sonenberg M, Rawson RW. The relation of radioiodine dosimetry to results and complications in the treatment of metastatic thyroid cancer. *AJR Radium Ther Nucl Med.* 1962;87:171–182.
21. Summary of current radiation dose estimates to humans from ^{123}I, ^{124}I, ^{125}I, ^{126}I, ^{130}I, ^{131}I, and ^{132}I as sodium iodide. *J Nucl Med.* 1975;16:857–860.
22. International Commission on Radiological Protection. *Radiation Dose to Patients from Radiopharmaceuticals.* New York, NY: Pergamon Press; 1988:275. ICRP publication 53.
23. Berman M, Hoff E, Barandes M, et al. Iodine kinetics in man: a model. *J Clin Endocrinol Metab.* 1968;28:1–14.
24. Johansson L, Leide-Svegborn S, Mattsson S, et al. Biokinetics of iodide in man: refinement of current ICRP dosimetry models. *Cancer Biother Radiopharm.* 2003;18:445–450.
25. Edmonds CJ, Smith T. The long-term hazards of the treatment of thyroid cancer with radioiodine. *Br J Radiol.* 1986;59:45–51.
26. Smith T, Edmonds CJ. Radiation dose in the treatment of thyroid carcinoma by ^{131}I. *Radiat Prot Dosimetry.* 1984;5:141–149.

JNM The Journal of NUCLEAR MEDICINE

Prediction of Absorbed Dose to Normal Organs in Thyroid Cancer Patients Treated with ^{131}I by Use of ^{124}I PET and 3-Dimensional Internal Dosimetry Software

Katherine S. Kolbert, Keith S. Pentlow, Joel R. Pearson, Arif Sheikh, Ronald D. Finn, John L. Humm and Steven M. Larson

J Nucl Med. 2007;48:143-149.

The Journal of Nuclear Medicine is published monthly.
SNMMI | Society of Nuclear Medicine and Molecular Imaging
1850 Samuel Morse Drive, Reston, VA 20190.
(Print ISSN: 0161-5505, Online ISSN: 2159-662X)

SNMMI SOCIETY OF NUCLEAR MEDICINE AND MOLECULAR IMAGING